J Oral Pathol Med (2005) 34: 498–507

www.blackwellmunksgaard.com/jopm

Extracellular matrix remodeling in oral submucous fibrosis: its stage-specific modes revealed by immunohistochemistry and *in situ* hybridization

Hiroko Utsunomiya[1], Wanninayake M. Tilakaratne[1,2], Kazufumi Oshiro[1], Satoshi Maruyama[1], Makoto Suzuki[1], Hiroko Ida-Yonemochi[1], Jun Cheng[1], Takashi Saku[1]

[1]*Division of Oral Pathology, Department of Tissue Regeneration and Reconstruction, Niigata University Graduate School of Medical and Dental Sciences, Niigata, Japan;* [2]*Department of Oral Pathology, Faculty of Dental Sciences, University of Peradeniya, Peradeniya, Sri Lanka*

BACKGROUND: Oral submucous fibrosis (OSF) is a chewing habit-related pre-cancerous condition of the oral mucosa affecting predominantly south Asians. It is histopathologically characterized by epithelial atrophy and fibrosis of the subepithelial connective tissue. Fibrosis extends all the way into the muscle layer, leading to difficulty in mouth opening. However, the dynamics of extracellular matrix (ECM) remodeling with OSF progression is largely unknown.

METHODS: Forty biopsy specimens of OSF and 10 of normal buccal mucosa were examined for expression/deposition modes of eight ECM molecules by histochemistry, immunohistochemistry, and *in situ* hybridization.

RESULTS: In the early stage of OSF, tenascin, perlecan, fibronectin, collagen type III were characteristically enhanced in the lamina propria and the submucosal layer. In the intermediate stage, the ECM molecules mentioned above and elastin were extensively and irregularly deposited around muscle fibers. In the advanced stage, such ECM depositions decreased and were entirely replaced with collagen type I only. Their gene expression levels varied with progression of fibrosis, but the mRNA signals were confirmed in fibroblasts in the submucosal fibrotic areas.

CONCLUSIONS: The results indicate that the ECM remodeling steps in OSF are similar to each phase of usual granulation tissue formation. Restricted mouth opening may be a result of loss of variety of ECM molecules including elastin into the homogeneity of collagen type I replacing muscle fibers.

J Oral Pathol Med (2005) **34**: 498–507

Correspondence: Takashi Saku, Division of Oral Pathology, Department of Tissue Regeneration and Reconstruction, Niigata University Graduate School of Dental Sciences, 2-5274 Gakkocho-dori, Niigata 951-8514, Japan. Tel.: 81 (25) 2272832. Fax: 81 (25) 2270805. E-mail: tsaku@dent.niigata-u.ac.jp
Accepted for publication April 5, 2005

Keywords: collagen; elastin; extracellular matrix (ECM) molecules; oral submucous fibrosis; perlecan

Introduction

Oral submucous fibrosis (OSF) is a pre-cancerous condition predominantly seen among betel quid chewers in south Asian countries (1, 2). The disease was first reported in early 1950s, and its pre-cancerous condition was identified by Paymaster (3). It has characteristic clinical presentation depending on the stage of the disease, but the majority of the patients with OSF have intolerance to spicy foods, roughness of the oral mucosa, and different degrees of difficulty in opening the mouth (4). More attention has been paid to investigate the etiology/pathogenesis and malignant transformation in the epithelium of OSF (5–7), while connective tissue remodeling itself in the subepithelial fibrosis has not been so extensively studied from a histopathologic point of view. Thus, a better understanding of the disease is required in terms of precise staging and progression not only by depth of fibrosis but also by more objective analysis of extracellular matrix (ECM), because the disease is basically manifested in the connective tissue.

There have been many investigations on the molecular mechanism for progression of OSF, especially for enhanced biosynthesis of collagen type I by fibroblasts due to the stimulation by betel quid ingredients (8–10) as well as the resistance of mature collagen fibrils against degradation (11). However, histological investigations of fibrosis in OSF, including immunohistochemical studies for ECM, have not been widely performed since Pindborg and Sirsat reported four distinct disease phases in 1966 (12). It is of utmost important to identify the disease as early as possible in order to prevent its possible malignant transformation in it. However, it is

not always easy to evaluate subjectively the progression stages of OSF, because its early histopathological features are not pathognomonic. Thus, the identification of ECM remodeling characteristics may help to diagnose the disease early and properly.

Our intent in this study, therefore, was to examine different kinds of ECM molecules, which may be involved in the progression of the disease and to determine the cell types, which are responsible for the metabolism of those ECM molecules in order to understand more clearly the background for the pathogenesis of the inability of mouth opening. It is important to understand the ECM remodeling mechanism in OSF, as it is a common pre-cancerous condition of the oral mucosa. Recently, hypoxia has attracted much attention as one of the important backgrounds for carcinogenesis (13). The development of epithelial malignancy in OSF may be partly explained by the hypothesis, because hypoxic conditions of the oral mucosal epithelium should be generated by extensive and long-standing submucous fibrosis.

Materials and methods

Materials

Forty biopsy specimens of OSF were selected from the surgical pathology files of the Department of Oral Pathology, Faculty of Dental Sciences, University of Peradeniya, Sri Lanka during a 2-year period from 2001 to 2003. Intra-oral sites of the specimens of OSF taken were as follows: buccal mucosa, 35; tongue, 4; lip, 1. As controls, 10 samples of normal buccal mucosa were selected from the surgical pathology files of the Division of Oral Pathology, Niigata University Graduate School of Medical and Dental Sciences. All the specimens were routinely fixed in 10% formalin and embedded in paraffin blocks. Serial 5-μm sections were cut from paraffin blocks. One set of the sections was stained with hematoxylin and eosin (H&E) and was used for reevaluation of histological diagnosis, and the other sets were used for Orcein-Giemsa stain, Gomori's aldehyde fuchsin stain, and for immunohistochemistry and *in situ* hybridization.

Antibodies

Antibodies against perlecan, a basement membrane-type heparan sulfate proteoglycan, core protein (14), and fibronectin (15) were raised in rabbits as described elsewhere. Rabbit polyclonal antibodies against tenascin and collagen type I (type I) were purchased from Chemicon International Inc. (Temecula, CA, USA). Rabbit polyclonal antibodies against elastin and collagen type III (type III) were obtained from LSL Inc. (Tokyo, Japan). Rabbit polyclonal antibodies against collagen type IV (type IV) were obtained from Cappel Laboratories (Cochranville, OH, USA). Rabbit polyclonal antibodies against laminin were prepared as described elsewhere (16).

Immunohistochemistry

Serial paraffin sections were subjected to immunohistochemical staining for ECM molecules, such as perlecan, fibronectin, tenascin, types I, III, and IV, laminin, and elastin by using the Chemomate Envision/HRP system (Dako). For perlecan, tenascin, fibronectin, types I and III, deparaffinized sections were pre-treated with 3 mg/ml hyaluronidase (bovine testicular origin, type I-S, 440 U/mg; Sigma Chemical Co., St. Louis, MO, USA) in phosphate-buffered saline (PBS) for 30 min at 37°C. For type IV, laminin, and elastin, the sections were pre-treated with 0.02% trypsin (type II, Sigma) in 0.5 M Tris–HCl (pH 7.6) containing 1% $CaCl_2$ in 30 min at 37°C. Prior to incubation with the primary antibodies, all the sections were treated with 0.3% hydrogen peroxide in absolute methanol for 30 min at room temperature to block endogenous peroxidase activities. For blocking non-specific protein binding, sections were incubated with 5% skimmed milk for 1 h at 37°C after rinsing in PBS containing 0.5% skimmed milk and 0.05% Triton X-100 (T-PBS). They were then incubated overnight at 4°C with the primary antibodies diluted in T-PBS. For visualization of reaction products, sections were treated with 0.02% 3,3′-diaminobenzidine in 0.05 M Tris–HCl buffer (pH 7.4) containing 0.005% hydrogen peroxide. The sections were counterstained with hematoxylin. For control studies, the primary antibodies were replaced with pre-immune rabbit IgG.

Preparation of RNA probes

All the mRNA probes for *in situ* hybridization were prepared with *in vitro* transcription with PCR products of RNA samples of normal oral mucosa as previously described (17) and primer sets as shown in Table 1. A template of cDNA corresponding to a fragment of each molecule was amplified by reverse transcription polymerase chain reaction (RT-PCR) using the RNA samples. The PCR products were subcloned into plasmid vectors and were digested with appropriate restriction enzymes as shown in Table 1. The linearized plasmids were used as templates to synthesize digoxigenin (DIG) labeled RNA anti-sense and sense probes using labeling kits, including 5-Bromo-4-chloro-3-indolyl-phosphate (BCIP)/4-Nitro-blue tetrazolium chloride (NBT) as substrates, (F. Hoffmann-La Roche Ltd., Basel, Switzerland) and T7/T3 RNA polymerases (Promega Corporation, Madison, WI, USA), respectively.

In situ *hybridization*

In situ hybridization was performed as previously described (18). In short, after deparaffinization, sections were washed in three changes of 2× standard saline citrate (SSC) and treated with 5 μg/ml proteinase K (Sigma) for 20 min at 37°C. They were then washed with 0.2% glycine in PBS, fixed with 4% paraformaldehyde in 0.1 M phosphate buffer (pH 7.5) for 30 min, dehydrated with a series of ethanol (70–100%), and air dried. Hybridization was performed at 45°C for 16 h in a moist chamber. The hybridization solution contained 10 mM phosphate buffer (pH 7.4), 10% dextran sulfate, 1× Denhardt's solution, 100 μg/ml salmon sperm DNA, 125 μg/ml yeast tRNA, 3× SSC, 50% formamide, and 500 ng/ml probes. After hybridization, the sections were rinsed in 2× SSC, and then the hybridized probes were

Table 1 The mRNA probes used for *in situ* hybridization

Molecule	*Primer sequence*	*Probe size (base number)*	*Genbank accession number*	*Subcloned vector*	*Digestion*
Collagen type I					
Sense	5′-CTGGCAAAGAAGGCGGCAAA-3′	503 bp (1430–1932)	K01228	pGEM-Teasy	*Sal*I
Anti-sense	5′-CTCACCACGATCACCACTCT-3′				*Sal*I
Collagen type III					
Sense	5′-GATATTGCTATCAGTAGGCTGGTG-3′	342 bp (4429–4770)	X14420	pGEM-Teasy	*Nco*I
Anti-sense	5′-GTTGAAGTTTATTTATTATAGCACC-3′				*Sal*I
Collagen type IV					
Sense	5′-GCTCACCAGGACCAGTGGGT-3′	310 bp (2802–3111)	XM-049913	pGEM3Z	*Hin*dIII
Anti-sense	5′-TCACCTTTAGGTCCTGGCTG-3′				*Sal*I
Fibronectin					
Sense	5′-GCCTGGTACAGAATATGTAGTG-3′	421 bp (3907–4327)	X02761	pGEM-Teasy	*Nco*I
Anti-sense	5′-ATCCCAGCTGATCAGTAGGCTGGTG-3′				*Sal*I
Elastin					
Sense	5′-CGGGATCCGCTATGGACTGCCCTACACC-3′	305 bp (646–951)	M36860	pBluescript IIKS+/−	*Eco*RI
Anti-sense	5′-CGGAATTCCATACTTGGCTGCCTTAGC-3′				*Bam*HI
Tenascin					
Sense	5′-CCCAAGCTTTGGAGTCTGCA-3′	204 bp (834–1037)	55618	pSPT18/19	*Hin*dIII
Anti-sense	5′-GGAATTCCACACGCACTCAT-3′				*Eco*RI
Perlecan					
Sense	5′-CTGCTGGCGGTGACCCATGG-3′	516 bp (135–669)	NM005529	pBluescript IIKS+/−	*Bam*HI
Anti-sense	5′-TTGGGAACTGGGGCACTGTG-3′				*Hin*dIII
Laminin					
Sense	5′-GAATCAGAATGGCTGGTAACATTTG-3′	319 bp (7613–7931)	X58531	pGEM-Teasy	*Sal*I
Anti-sense	5′-CTAATGTGCCCAACTTCATTTCC-3′				*Nco*I

detected with DIG detection kits (alkaline phosphatase; Roche). The sections were counterstained with methyl green.

Histopathological evaluation

Using HE-stained sections, all the OSF cases were classified into three stages, early, intermediate, and advanced, by basically following the concept of Pindborg and Sirsat (12), which is based on the degree of inflammatory cell infiltration and fibrosis. As for the epithelial changes, the cases were classified into normal, hyperplasia, and different grades of epithelial dysplasia. For these histological evaluations, the special stainings mentioned above were used to confirm some specific findings of OSF in relation to extracelluar matrix remodeling.

Results

Histopathology

A total of 59 areas among the 40 cases were evaluated histopathologically. They were classified into three different stages. According to our evaluation, 9 areas were classified into the early stage, 26 into the intermediate stage, and 23 into the advanced stage, respectively. A majority of cases showed atrophic changes in the epithelium with thinning and loss of rete ridges. Some cases had vacuolation of epithelial cells, especially in the basal or parabasal cell layers. Frequently observed dysplastic changes consisted of irregular basal cell alignment and budding-like shapes of rete processes. Occasional cases showed spongiosis in prickle cells.

In the subepithelial connective tissue, histological features were varied with the progress of the disease. In the early stage, a large number of lymphocytes were present in the immediate subepithelial zone corresponding to the lamina propria with myxoedematous changes but not yet with significant fibrotic changes (Fig. 1a). In the intermediate stage, granulation changes extended close to the muscle layer, and hyalinization began to appear in the subepithelial zone, where blood vessels were compressed by thick fibrous bundles. Although inflammatory cells were reduced in number in the submucosal layer, they began to appear in myxoedematous surrounding areas of the muscle layer (Fig. 1b). In the advanced stage, inflammatory cell infiltrations were hardly seen and the number of vessels became dramatically small in the subepithelial zone. Marked fibrosis areas with hyaline changes were widely seen from the subepithelial to superficial muscle layers. When there was creeping fibrosis into the muscle layers, atrophic, and degenerative changes started to appear in muscle fibers. However, occasional cases showed persistent foci of inflammatory cells around muscle fibers. Some cases of the advanced stage showed focal inflammatory cell infiltrations in the subepithelial layer, which appeared to be revived inflammatory processes in the area which had been previously organized (Fig. 1c).

Aldehyde fuchsin and orcein-Giemsa stains revealed regular modes of distribution of elastic fibers in normal mucosa. They were arranged in a faint band-like fashion in the interface between the lamina propria and the submucosal layer, which were almost parallel to the epithelial layer. In the muscle layer, elastic fibers circumscribed each muscle fiber. Elastic fibers were also found in the surroundings of muscular blood vessels (Fig. 2a). In OSF, elastic fibers were irregularly arranged in the lower submucosal layer as well as in the muscle layer in the early stage (Fig. 2b). In the intermediate stage, there were many

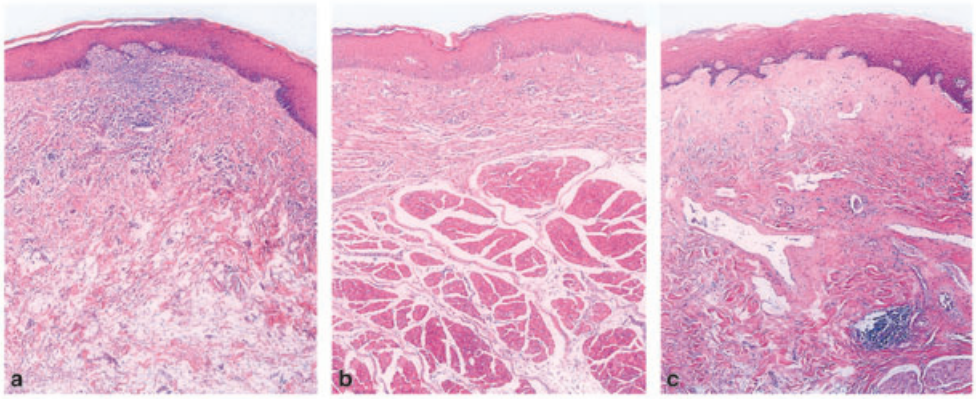

Figure 1 Histopathological appearance of oral submucous fibrosis (OSF) in three stages: early (a), intermediate (b), and advanced (c) stages (HE stain, ×40). The early stage is characterized by myxoedematous changes of the immediate subepithelial zone corresponding to the lamina propria with a diffuse infiltration of lymphocytes but not yet with significant fibrotic changes (a). In the intermediate stage, fibrotic changes extended close to the muscle layer, and hyalinization began to appear in the subepithelial zone (b). In the advanced stage, there were extensive fibrotic areas with hyaline changes from the subepithelial to muscle layers (c).

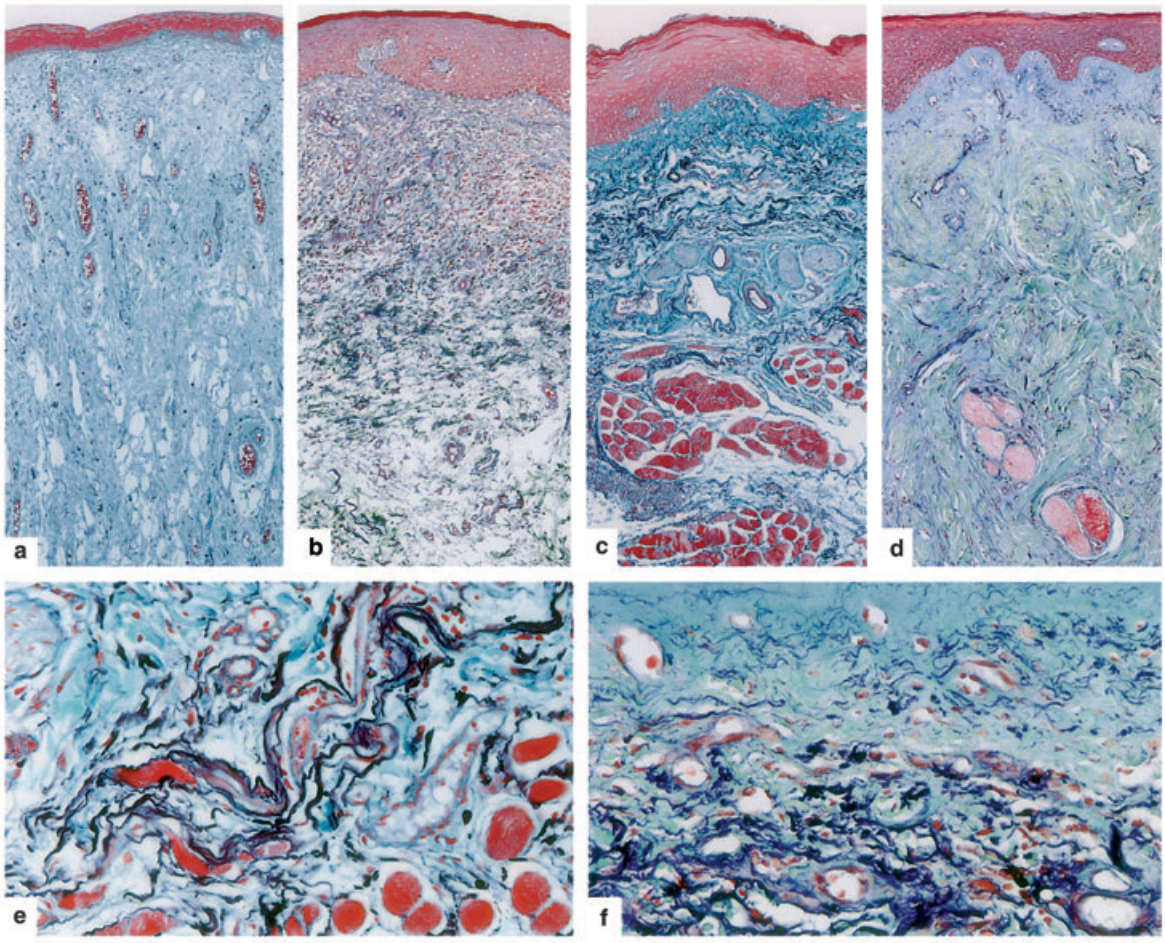

Figure 2 Distribution modes of elastic fibers in oral submucous fibrosis (OSF). (a) normal mucosa, (b) early, (c) intermediate, and (d) advanced stages of OSF. High-power view of the muscle layer (e) and of submucosal layer (f) in the intermediate phase (Aldehyde fuchsin stain; a–d, ×60; e, ×200; f, ×250). In normal mucosa, aldehyde fuchsin positive fibers or elastic fibers are minimal in the lamina propriae to the submucosal layer (a). In the early stage of OSF, fine, and short elastic fibers were irregularly arranged in the lower submucosal layer (b). In the intermediate stage, there were significant amounts of elastic fibers in an irregular fashion around atrophic muscle fibers (c). Around the degenerated muscle fibers, thick, and long elastic fibers were stacked on each other to form irregular shaped bundles with various thicknesses (e). In the later phase of the intermediate stage, elastic fibers gradually disappeared with the extension of fibrosis and hyalinization (f). In the advanced stage, elastic fibers disappeared completely from the extensive fibrotic areas (d).

and thick elastic fibers anastomosed irregularly around degenerated muscle fibers (Fig. 2c, e). However, the above feature disappeared when fibrosis and hyalinization progressed into the advanced stage (Fig. 2d, f).

Immunohistochemistry and in situ *hybridization*

Immunohistochemical staining and *in situ* hybridization for eight ECM molecules were performed.

Tenascin

Tenascin was immunolocalized in a band-like fashion beneath the epithelial basement membrane (BM), called the BM zone in the following section, in the early stage (Fig. 3b). However, such a tenascin band-like immunopositivity disappeared completely in the intermediate (Fig. 3c) and advanced (Fig. 3d) stages. The mRNA signals for tenascin were faintly detected in the basal cells of the oral epithelium and fibroblasts in the juxtaepithelial zone in the early stage (Fig. 3e). In the intermediate and advanced stages, however, there was no expression of mRNA for tenascin either in epithelial cells or in subepithelial connective tissues. In control experiments using pre-immune IgG or sense probes, there were no positive reactions.

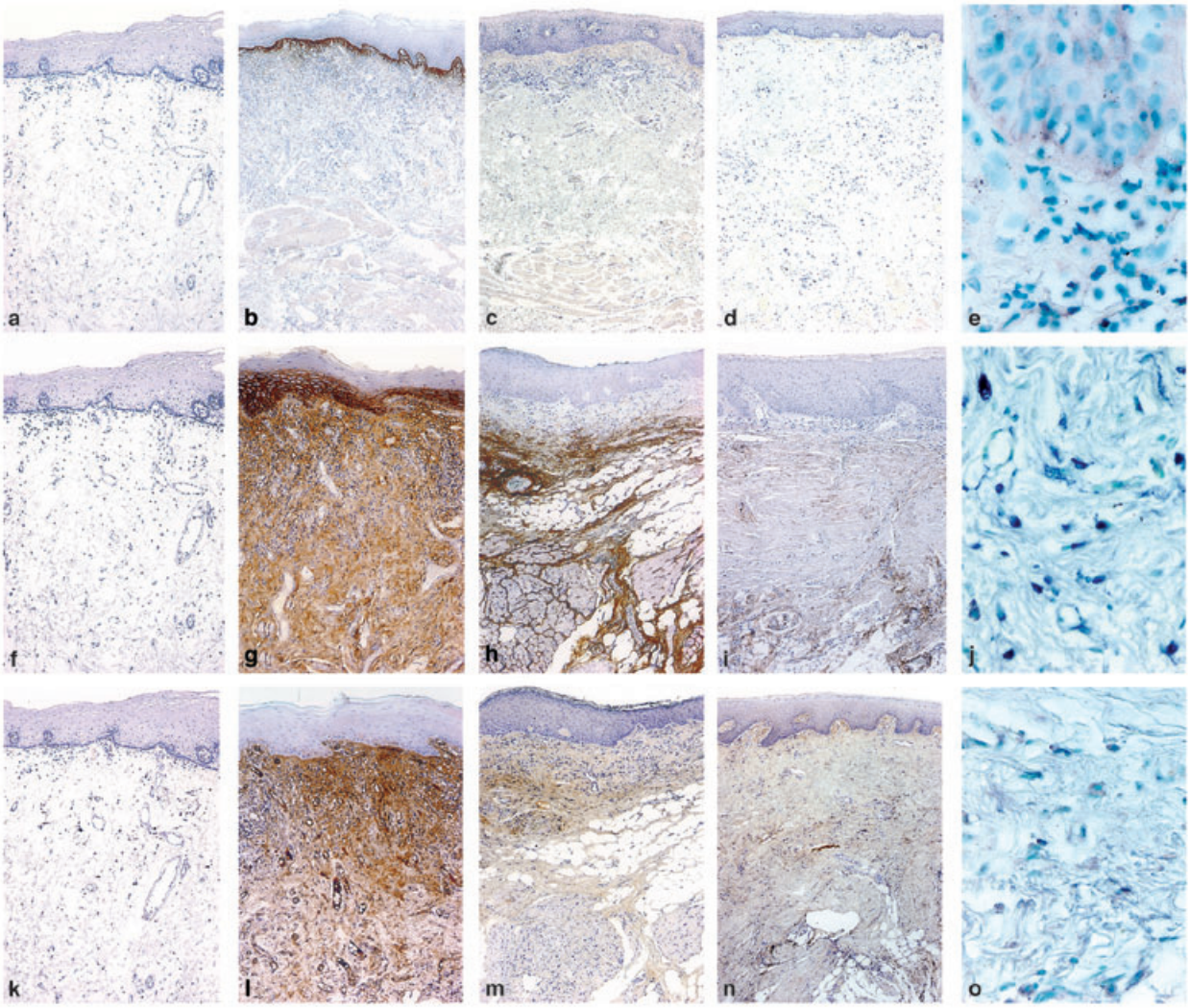

Figure 3 Immunohistochemistry and *in situ* hybridization for ECM molecules in oral submucous fibrosis (OSF) (I). Immunoperoxidase stain for tenascin (a–d), perlecan (f–i), fibronectin (k–n), hematoxylin counterstain and *in situ* hybridization for tenascin mRNA in the early stage of OSF (e), perlecan (j), and fibronectin (o) mRNA in the intermediate stage of OSF, digoxygenin-alkaline phosphatase, methyl green counterstain. (a, f, k) normal mucosa; (b, g, l) early; (c, h, m) intermediate; (d, i, n) advanced stages (a, f, k, ×50; b–d, g–i, l–n, ×40; e, j, o, ×300). Tenascin was immunolocalized in the basement membrane (BM) zone of the epithelium in the early stage (b), but its immunopositivity disappeared with the advance of stages from the intermediate (c) to advanced (d). The mRNA signals for tenascin (e) were faintly detected in the basal to parabasal cells of the epithelium as well as in fibroblasts in the subepithelial zone in the early stage. Perlecan was immunopositive in the lamina propria to the submucosal layer, in addition to the lower epithelial layers, in the early stage (g), while the staining intensity became weaker in the lamina propriae (h), and its positivity became stronger in the submucosal and muscle layers in the intermediate stage. In the advanced stage, however, most of the immunolocalization for perlecan disappeared from the superficial fibrotic layer, leaving some immunopositive areas in the muscle layer (i). mRNA signals for perlecan were detected in fibroblasts which increased in number with the extension of myxoedematous changes in the lamina propriae to the submucosal layers in the early stage (j). The immunolocalization for fibronectin was similar to that of perlecan (l–n). The mRNA signals for fibronectin were localized in activated fibroblasts in the same pattern as those for perlecan in the early stage (o).

Perlecan

Perlecan, a basement membrane type heparan sulfate proteoglycan, was strongly and diffusely immunopositive from the lamina propria to the submucosal layer, which showed a myxoedematous appearance in HE-stained sections in the early stage (Fig. 3g). The mRNA signals for perlecan were detected in fibroblasts, which increased in number with the extension of myxoedematous changes from the lamina propria to the submucosal layer. The signals were also detected in vascular endothelial cells and in inflammatory cells, such as lymphocytes and macrophages. In the intermediate stage, the staining intensity for perlecan became weaker in the lamina propria, however, it became stronger in the submucosal layer. The immature granulation tissue with inflammatory cell infiltrations around the muscle layer also showed various degrees of immunopositivities for perlecan (Fig. 3h). Activated fibroblasts showed definite mRNA signals, indicating that they were major responsible cells for perlecan (Fig. 3j). In the advanced stage, the immunolocalization for perlecan disappeared from the subepithelial zone. In contrast, the muscle layer showed immunopositive for perlecan (Fig. 3i). Perlecan was immunolocalized not only in the basement membrane of muscle fibers but also in the widened interfascicular space, which was due to granulation formation. With the progress of fibrosis into the advanced stage, the number of fibroblasts, which expressed mRNA signals for perlecan, became less, and finally there were no fibroblasts expressing any mRNA signals in completely fibrosed areas.

Fibronectin

The immunolocalization of fibronectin showed the same tendencies as those of perlecan. In the early stage, it was localized diffusely in the lamina propria and in the submucosal layer (Fig. 3l). The mRNA signals for fibronectin were mainly found in interstitial fibroblasts but definitely not in vascular endothelial cells or inflammatory cells, which also had perlecan mRNA expression. With the progression of fibrosis, fibronectin deposits were shifted to the deeper area leaving some trace in the subepithelial zone. In the intermediate stage, they were most predominantly seen around damaged muscle fibers (Fig. 3m). The mRNA signals for fibronectin were localized in activated fibroblasts in the same pattern as those for perlecan (Fig. 3o). In the advanced stage, there was no fibronectin in densely fibrosed areas but only around atrophic muscle fibers scattered in the fibro-hyaline tissue (Fig. 3n). Its genes were scarcely expressed in fibroblasts within the dense fibrous tissue.

Collagen type III

Type III showed a diffuse and moderate immunopositivity within the lamina propria as well as in the submucosal layer in the early stage (Fig. 4b), while it was not evident in any layers of normal mucosa (Fig. 4a). In the intermediate stage, it was more strongly immunolocalized in fibrous granulation tissue (Fig. 4c). No significant expression in the interstitium of the muscle layer, although Fig. 4c showed non-specific staining within the muscle fibers. With the advancement of the disease, type III expression became weaker and was lost completely in the advanced stage (Fig. 4d). The mRNA signals for type III were also detected in fibroblasts, but the signal intensities were not as strong as those for other ECM molecules (Fig. 4e). With the progress of the disease, its mRNA signals in fibroblasts became fewer and were lost completely in advanced fibrosis.

Collagen type I

In contrast to the tendency for type III described above, the expression modes of type I showed dramatic relationships with the progression stages of the disease. In normal mucosa, type I was faintly and diffusely immunolocalized in the lamina propria and the interstitium of any layers (Fig. 4f). In the early stage, type I was immunolocalized only in the lamina propria in a weak and scattered pattern (Fig. 4g). However, it extended to the submucosal layer in a diffuse sheet-like appearance in the intermediate stage (Fig. 4h). Finally, type I was seen strongly positive in the whole area of the fibrosis (Fig. 4i). The mRNA signals for type I were detected in fibroblasts in all stages (Fig. 4j). In the early stage, its signals were stronger and more frequently seen in the lamina propria than in the submucosal layer. In the intermediate stage, there were strong mRNA signals in fibroblasts in the lower submucosal layer, but the distribution of fibroblasts was irregular. In the advanced stage, not only the number of fibroblasts became less but also the signal intensities for type I mRNA in fibroblasts were decreased, in contrast to its strong and diffuse immunolocalization in the fibrosed area.

Elastin

The expression of elastin showed a significant correlation with the advancement of the disease. In normal mucosa, it was only immunolocalized around blood vessels and muscle fascicles (Fig. 4k). In the early stage, elastin was expressed moderately in the deeper parts of the submucosa and in the connective tissue surrounding muscles (Fig. 4l). The mRNA signals for elastin were faintly seen in the fibroblasts. In the intermediate stage, the strongest immunolocalization for elastin occurred in an irregular pattern in the subepithelial zone down to the muscle layer (Fig. 4m). Its staining pattern was patchy or diffuse and irregular in thickness when it was in a linear fashion. The staining intensity for elastin became almost non-existent when the total area became fibrosed (Fig. 4n). The mRNA signals for elastin characteristically increased in fibroblasts that were present in the middle to lower subepithelial zone as well as in the granulation tissues surrounding muscles in the intermediate to early advanced stages. Fibroblasts in the fibrous tissue around degenerated muscle fibers showed the strongest mRNA expression levels for elastin (Fig. 4o). However, in the late advanced stage, the signals for elastin decreased dramatically and were not found in fibroblasts in completely fibro-hyaline areas.

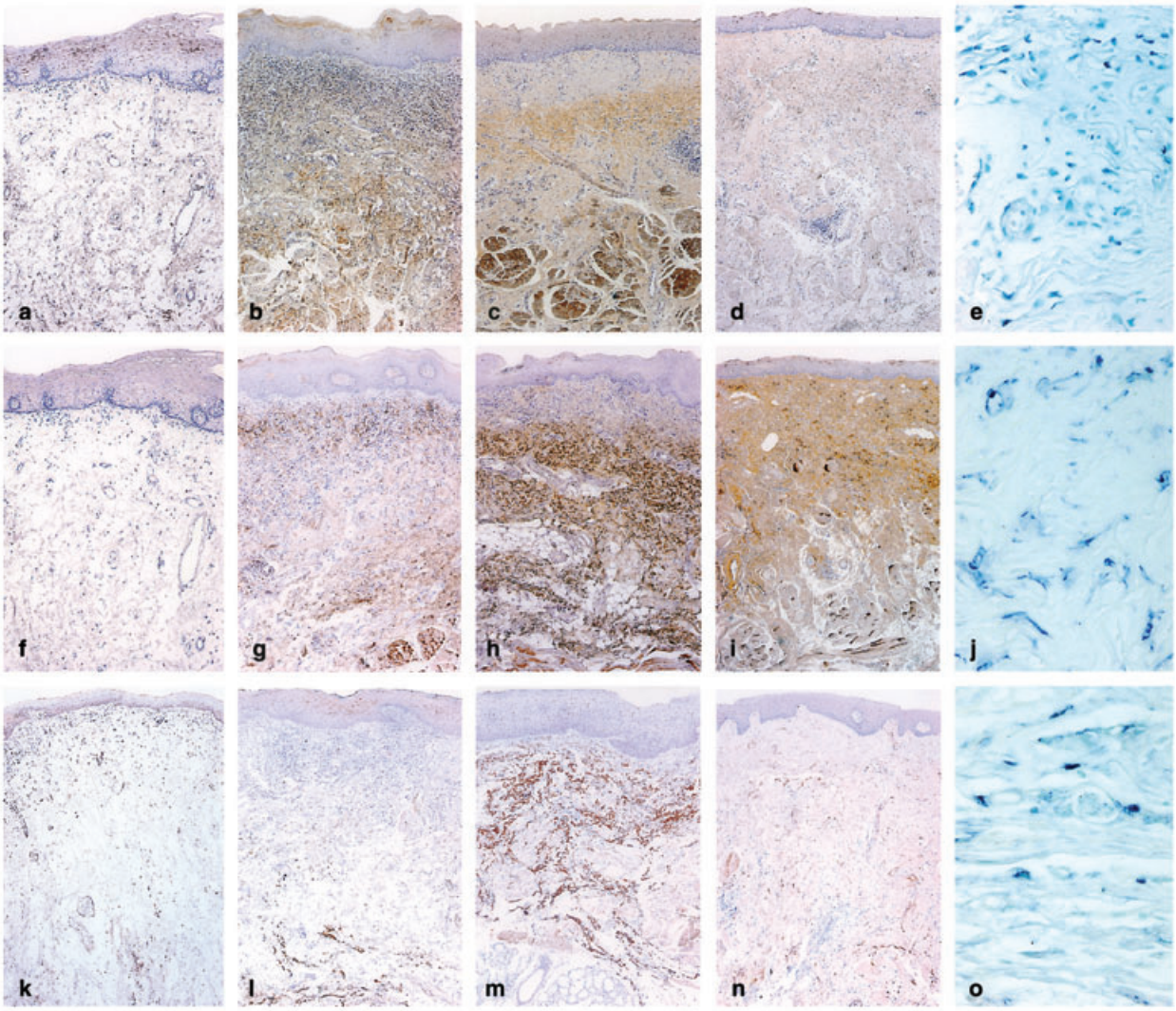

Figure 4 Immunohistochemistry and *in situ* hybridization for ECM molecules in oral submucous fibrosis (OSF) (II). Immunoperoxidase stain for collagen type III (a–d), collagen type I (f–i), and elastin (k–n), hematoxylin counterstain and *in situ* hybridization for collagen type III (e), collagen type I (j), and elastin (o) mRNAs in the intermediate stage, digoxygenin-alkaline phosphatase, methyl green counterstain. (a, f, k) normal mucosa; (b, g, l) early; (c, h, m) intermediate; (d, i, n) advanced stages (a, f, k, ×50; b–d, g–i, l-n, ×40; e, j, o, ×300). Collagen type III was immunolocalized diffusely and moderately in the lamina propria to the submucosal layer in the early stage (b). With the advancement of the disease, type III expression became weaker (c), and was lost completely in the advanced stage (d). mRNA signals for type III were also detected in fibroblasts in the fibrotic areas, but their signal intensities were not as strong as those for other ECM molecules (e). The immunolocalization for collagen type I extended with the progress of the disease in a diffuse fashion from the submucosal layer to both the surface and profound zones (g–i). The mRNA signals for type I were detected in fibroblasts in all the stages (j). Elastin was immunolocalized only around the vascular channels and muscle fibers in normal mucosa (k). In the early stage, the immunolocalization for elastin was enhanced in the peri-muscular area and it became strongest and irregular in the subepithelial zone to the muscle layer in the intermediate stage (m). However, the elastin immunolocalization disappeared mostly when the submucous area became totally fibrotic (n). Fibroblasts around degenerated muscle fibers showed the strongest signals for elastin mRNA (o).

Laminin and collagen type IV

Type IV and laminin were mainly immunolocalized in the epithelial, muscular, and blood vascular basement membranes (data not shown). Their immunolocalization patterns did not show significant changes through different stages of OSF and were similar to those in the normal mucosal tissues.

The ratios of immunopositivities for the eight ECM molecules in each stage mentioned above were summarized in Table 2. All of the tendencies for remodeling of ECM molecules with the progress of the disease were schematically graphed with regard to different areas of the subepithelial space in Fig. 5. It is clear from the schemes that each molecule expressed itself quite differently from other molecules not only in different phases but also in the different area through the progress of the disease and that their dynamic expression modes were site- and stage-specific.

Discussion

The present study demonstrated clearly the differential expression of eight ECM molecules at their gene and

Table 2 Expression modes of extracellular matrix (ECM) molecules in each stage of oral submucous fibrosis (OSF)

	Immunopositivities (%) for ECM molecules among examined cases							
Oral mucosal layers	*Tenascin*	*Perlecan*	*Fibronectin*	*Type I*[a]	*Type III*[a]	*Type IV*[a,b]	*Laminin*[b]	*Elastin*
Early stage (9 samples)								
BM-zone	78	22	33	22	33	100	100	0
Lamina propria	0	78	78	33	56	100	89	11
Submucosa	0	78	89	33	67	100	96	78
Muscle	0	0	0	0	0	100	100	89
Intermediate stage (26 samples)								
BM-zone	35	46	54	69	19	100	92	0
Lamina propria	0	31	35	65	27	100	96	15
Submucosa	0	69	69	62	31	100	96	92
Muscle	0	31	35	31	27	100	100	96
Advanced stage (23 samples)								
BM-zone	9	4	9	78	4	100	100	0
Lamina propria	0	9	9	100	9	100	100	9
Submucosa	0	15	22	87	9	100	89	17
Muscle	0	30	17	91	9	100	96	13

[a]Collagen types I, III, and IV.
[b]Mainly in epithelial, muscular, and blood vascular basement membranes.

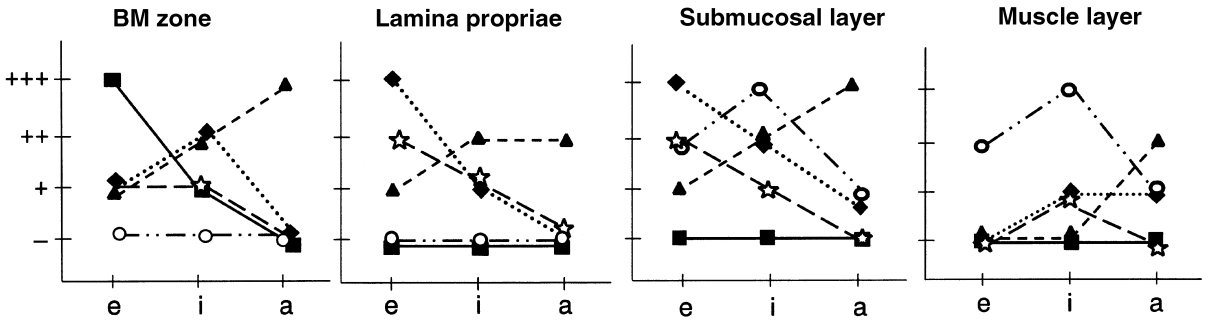

Figure 5 Schematic modes of extracellular matrix (ECM) remodeling in oral submucous fibrosis (OSF) summarize in every four layers from the basement membrane (BM) zone, lamina propriae, submucosal layer, and muscle layer. ■, tenascin, ◆, perlecan and fibronectin, ▲, collagen type I, ☆, collagen type III, ○, elastin; (–) absent, (+) weak, (++) medium, (+++) strong; e, early stage, i, intermediate stage, a, advanced stages.

protein levels in the subepithelial connective tissue with the progress of OSF. This is the first trial and fundamental record of ECM dynamics in OSF, although OSF has been recognized as an abnormal ECM remodeling event since the disease entity was proposed 50 years ago (3). The expression of each ECM molecule appears to have a specific relationship with different stages of OSF, suggesting that at least six of the eight ECM molecules are associated with the progression of the disease at different stages. The results indicate that the progression of OSF stages can be regarded as a kind of maturation mode of granulation tissue.

The linear deposit of tenascin in the BM zone in the early stage of OSF and its production by basal cells in the oral epithelium were different from those of other ECM molecules. Reichart et al. has reported similar band-like immunohistochemical localization for tenascin in the advanced stage of OSF (19), although their observation was not always in a stage-based manner. These results suggest that the metabolism of tenascin is regulated mainly by keratinocytes or by keratinicyte–fibroblast interaction and that it plays an important role in formation and regulation of immature granulation tissues with myxoedematous appearances on HE-stained sections. Similar data have been already documented in oral wound healing (20). In addition, our present results indicated that tenascin is a variable marker for identification of the early stage of OSF, even when histological features are not yet very characteristic in terms of fibrosis.

Perlecan and fibronectin showed similar modes of immunolocalization and gene expression through the progress of the disease. These molecules were mainly immunopositive in immature granulation tissue that also had a myxoedematous appearance on HE-stained sections. Similar data have been reported for gastrointestinal tracts (21) and in oral granulation tissues (20, 22, 23). Since it was evident that the main area of inflammatory reaction moved from the upper submucosal layer to the lower muscle layer with the progress of the disease, the area of the strongest deposition of these ECM molecules also moved to the surrounding area of damaged muscle fibers. These results indicate that both perlecan and fibronectin are important factors for regulation of maturation of granulation tissues towards fibrosis in OSF. It is also emphasized that these two

ECM molecules were produced not only by fibroblasts but also by lymphoid cells, as already reported (24). The expression of perlecan and fibronectin has been suggested to be important in such immature granulation tissue, because they may activate lymphoid cells as well as stromal fibroblasts directly or indirectly by their binding capacities with cytokines (25).

Among the three types of collagen that were studied, the dramatic increase in deposition of type I, and the contrastive reduction of type III with the progress of OSF were noticeable. Similar findings to our results of reduction of type III with a concomitant increase in type I in the connective tissue of OSF specimens have already been observed by immunohistochemistry, and collagen type VI has been shown to undergo a fate similar to that of type III in OSF (19). More recent data indicate that types I and III may associate to form composite fibrils with type V collagen as a core on which types I and III are polymerized (26). The decline of type III indicates that this protein does not play an important role in fibrosis itself, while the cross-linking of type I-predominant collagen fibrils may be critical in the progress of fibrosis in OSF.

The most striking finding in the present study was the dynamic remodeling of elastin with the progression of OSF stages, which have not been documented in the literature. The present study disclosed for the first time that elastic fibers or elastin molecules are located in the lamina propria and around muscle fiber bundles in normal oral mucosa, where elastic fibers were mostly uniform in their length and arrangement. The dramatic increase of elastic fibers or elastin molecules in the intermediate stage and their complete loss in the advanced stage were very characteristic of OSF. The biosynthesis of elastin in normal oral mucosa as well as in OSF was shown to due to interstitial fibroblasts. From the present findings, it is evident that in addition to the damage of muscle fibers, reduction of elastic fibers also causes loss of elasticity and flexibility leading to difficulty in mouth opening in patients with OSF in the advanced stage.

In the advanced stage, collagen type I seem to be a sole and major ECM constituent in the entire zone of fibrosis, replacing other ECM molecules deposited in the early and intermediate stages. Although we did not investigate further this concentric replacement of various ECM molecules with type I in the present study, appropriate molecular interactions or cascades among degradation enzymes and their target ECM molecules are expected. Further, there may be combinations of anti-degradative molecules, such as tissue inhibitors metalloproteinase (TIMPs) for type I and enhanced biosynthesis of type I by fibroblasts (27). Finally, an increase in collagen cross-linkages might occur, thus rendering them more resistant to collagenase (28). Of course, the ingredients of betel quid, such as arecoline and arecardine from areca nuts (29) as well as nicotine from tobacco (30), may affect the process of metabolism of ECM molecules. Enhanced biosynthesis of collagen type I (10) as well as proliferation of fibroblasts (31) have been reported when they are exposed to arecoline and arecardine, although arecoline at higher concentrations markedly suppresses the proliferation of fibroblasts (32) and phagocytotic activities in fibroblasts (33). These studies indicate that arecoline and arecardine induce disproportion between synthesis and breakdown of collagen resulting in the accumulation of matured and old collagen fibers. In addition, lowered levels of collagenase activity have been shown in OSF (34).

Recently, increased levels of lysyl oxidase, which controls cross-linking of collagen and elastin fibrils in the presence of copper ions by catalyzing oxidative deamination of the ε-amino group in certain lysine and hydroxylysine residues (35), have been confirmed in fibroblasts in culture from OSF mucosal tissues of betel quid chewers (28). Collagen fibrils that are cross-linked by lysyl oxidase have been shown to be more resistant to digestion by mammalian collagenases (35). Trivedy et al. also demonstrated the correlation of the expression level of lysyl oxidase with regard to the progress of fibrosis (36). These findings would support the hypothesis that the accumulation of collagen fibers seen in advanced stages of OSF is not only due to overproduction of collagen type I but also due to a decrease in degradation of cross-linked collagen fibrils. However, there seems to be one other paradox: although elastin fibers also increased and elastin is converted from its soluble to insoluble forms by lysyl oxidase (35), the over-produced elastin is reduced and finally disappears in the gene and protein levels in the advanced stage. Since there has been no reasonable explanation for this phenomenon at the moment, more detailed investigation is needed to determine the elastin-specific metabolic pathway in the later stage of fibrosis.

In conclusion, it is suggested from the present study that OSF shows the feature of an organizing process of granulation tissue formed by oral mucosa due to chewing stimulation. In addition to type I collagen, other ECM molecules are also involved in the process. Therefore, these ECM molecules can be useful immunohistochemical markers for evaluating exact stages of OSF.

References

1. Reichert PA, Philipsen HP. *Betel and Miang. Vanishing Thai habits*. Bangkok: L White Lotus Co. Ltd., 1996; 11–52.
2. Gupta PC, Warnakulasuriya S. Global epidemiology of areca nut usage. *Addict Biol* 2002; **7**: 77–83.
3. Paymaster JC. Cancer of the buccal mucosa; a clinical study of 650 cases in Indian patients. *Cancer* 1956; **9**: 431–5.
4. Chiu CJ, Lee WC, Chiang CP, Hahn LJ, Kuo YS, Chen CJ. A scoring system for the early detection of oral submucous fibrosis based on a self-administered questionnaire. *J Public Health Dent* 2002; **62**: 28–31.
5. Pillai R, Balaram P, Reddiar KS. Pathogenesis of oral submucous fibrosis. Relationship to risk factors associated with oral cancer. *Cancer* 1992; **69**: 2011–20.
6. Murti PR, Bhonsle RB, Gupta PC, Daftary DK, Pindborg JJ, Mehta FS. Etiology ofvb oral submucous fibrosis with special reference to the role of areca nut chewing. *J Oral Pathol Med* 1995; **24**: 145–52.
7. Trivedy CR, Craig G, Warnakulasuriya S. The oral health consequences of chewing areca nut. *Addict Biol* 2002; **7**: 115–25.

8. Canniff JP, Harvey W. The aetiology of oral submucous fibrosis: the stimulation of collagen synthesis by extracts of areca nut. *Int J Oral Surg* 1981; **10**: 163–7.
9. Meghji S, Scutt A, Harvey W, Canniff JP. An in vitro comparison of human fibroblasts from normal and oral submucous fibrosis tissue. *Arch Oral Biol* 1987; **32**: 213–5.
10. Kuo MYP, Chen HM, Hahn LJ, Hsieh CC, Chiang CP. Collagen biosynthesis in human oral submucous fibrosis fibroblast culture. *J Dent Res* 1995; **74**: 1783–8.
11. Scutt A, Meghji S, Canniff JP, Harvey W. Stabilisation of collagen by betel nut polyphenols as a mechanism in oral submucous fibrosis. *Experientia* 1987; **43**: 391–3.
12. Pindborg JJ, Sirsat SM. Oral submucous fibrosis. *Oral Surg Oral Med Oral Pathol* 1966; **22**: 764–79.
13. Gatenby RA, Gillies RJ. Why do cancers have high aerobic glycolysis? *Nat Rev Cancer* 2004; **4**: 891–9.
14. Saku T, Furthmyr H. Characterization of the major heparan sulfate proteoglycan secreted by bovine aortic endothelial cells in culture: homology to the large molecular weight molecule of basement membranes. *J Biol Chem* 1989; **264**: 3514–23.
15. Cheng J, Irié T, Munakata R, et al. Biosynthesis of basement membrane molecules by salivary adenoid cystic carcinoma cells: an immunofluorescence and confocal microscopic study. *Virchows Arch* 1995; **426**: 577–86.
16. Kobayashi Y, Nakajima T, Saku T. Loss of basement membranes in the invading front of O-1N, hamster squamous cell carcinoma with high potential of lymph node metastasis: an immunohistochemical study for laminin and type IV collagen. *Pathol Int* 1995; **45**: 327–34.
17. Ikarashi T, Ida-Yonemochi H, Oshiro K, Cheng J, Saku T. Intraepithelial expression of perlecan, a basement membrane-type heparan sulfate proteoglycan reflects dysplastic changes of the oral mucosal epithelium. *J Oral Pathol Med* 2004; **33**: 87–95.
18. Kimura S, Cheng J, Toyoshima K, Oda K, Saku T. Basement membrane heparan sulfate proteoglycan (perlecan) synthesized by ACC3, adenoid cystic carcinoma cells of human salivary gland origin. *J Biochem* 1999; **125**: 406–13.
19. Reichart PA, Van Wyk CW, Becker J, Schuppan D. Distribution of procollagen type III, collagen type VI and tenascin in oral submucous fibrosis (OSF). *J Oral Pathol Med* 1994; **23**: 394–8.
20. Okuda K, Murata M, Sugimoto M, et al. TGF-beta1 influences early gingival wound healing in rats: an immunohistochemical evaluation of stromal remodeling by extracellular matrix molecules and PCNA. *J Oral Pathol Med* 1998; **27**: 463–9.
21. Ohtani H, Nakamura S, Watanabe Y, Mizoi T, Saku T, Nagura H. Immunocytochemical localization of basic fibroblast growth factor in carcinomas and inflammatory lesions of the human digestive tract. *Lab Invest* 1993; **68**: 520–7.
22. Murata M, Hara K, Saku T. Dynamic distribution of basic fibroblast growth factor during epulis formation: an immunohistochemical study in an enhanced healing process of the gingiva. *J Oral Pathol Med* 1997; **26**: 224–32.
23. Yamazaki M, Cheng J, Hao N, et al. Basement membrane-type heparan sulfate proteoglycan (perlecan) and low-density lipoprotein (LDL) are co localized in granulation tissues: a possible pathogenesis of cholesterol granulomas in jaw cysts. *J Oral Pathol Med* 2004; **33**: 177–84.
24. Metwaly H, Cheng J, Ida-Yonemochi H, Ohshiro K, Jen KY, Saku T. Vascular endothelial cell participation in formation of lymphoepithelial lesions (epi-myoepithelial islands) in lymphoepithe – lial sialadenitis (benign lymphoepithelial lesion). *Virchows Arch* 2003; **443**: 17–27.
25. Schonherr E, Hausser HJ. Extracellular matrix and cytokines: a functional unit. *Dev Immunol* 2000; **7**: 89–101.
26. Birk DE. Type V collagen: heterotypic type I/V collagen interactions in the regulation of fibril assembly. *Micron* 2001; **32**: 223–37.
27. Shieh DH, Chiang LC, Shieh TY. Augmented mRNA expression of tissue inhibitor of metalloproteinase-1 in buccal mucosal fibroblasts by arecoline and safrole as a possible pathogenesis for oral submucous fibrosis. *Oral Oncol* 2003; **39**: 728–35.
28. Ma RH, Tsai CC, Shieh TY. Increased lysyl oxidase activity in fibroblasts cultured from oral submucous fibrosis associated with betel nut chewing in Taiwan. *J Oral Pathol Med* 1995; **24**: 407–12.
29. Chang MC, Kuo MY, Hsieh CG, Lin SK, Jeng JH. Areca nut extract inhibits the growth, attachment, and matrix protein synthesis of cultured human gingival fibroblasts. *J Periodontal* 1998; **69**: 1092–7.
30. Tipton DA, Dabbous MK. Effects of nicotine on proliferation and extracellular matrix production of human gingival fibroblasts in vitro. *J Periodontal* 1995; **66**: 1056–64.
31. Jeng JH, Kuo ML, Hahn LJ, Kuo MYP. Genotoxic and non-genotoxic effects of betel quid ingredients on oral mucosal fibroblasts in vitro. *J Dent Res* 1994; **73**: 1043–9.
32. Van Wyk CW, Olivier A, Hoal-Van Helden EG, Grobler-Rabie AF. Growth of oral and skin fibroblasts from patients with oral submucous fibrosis. *J Oral Pathol Med* 1995; **24**: 349–53.
33. Tsai CC, Ma RH, Shieh TY. Deficiency in collagen and fibronectin phagocytosis by human buccal mucosa fibroblasts in vitro as a possible mechanism for oral submucous fibrosis. *J Oral Pathol Med* 1999; **28**: 59–63.
34. Shieh TY, Yang JF. Collagenase activity in oral submucous fibrosis. *Proc Natl Sci Counc Repub China B* 1992; **16**: 106–10.
35. Kagan HM, Li W. Lysyl oxidase: properties, specificity, and biological role inside and outside of the cell. *J Cell Biochem* 2003; **88**: 660–72.
36. Trivedy C, Warnakulasuriya KAAS, Hazarey VK, Tavassoli M, Sommer P, Johnson NW. The upregulation of lysyl oxidase in oral submucous fibrosis and squamous cell carcinoma. *J Oral Pathol Med* 1999; **28**: 246–51.

Acknowledgment

This work was supported in part by Grants-in-Aid for Scientific Research from the Japan Society for the Promotion of Science.